

Preparation of Superionic Ceramics by Spark Plasma Method

Tomas ŠALKUS^{1*}, Ints STEINS², Maud BARRE³, Algimantas KEŽIONIS¹,
Antanas Feliksas ORLIUKAS¹

¹ Faculty of Physics, Vilnius University, Saulėtekio 9/3, LT-10222 Vilnius, Lithuania

² Institute of Inorganic Chemistry, Riga Technical University, Miera iela 34, LV-2169 Salaspils, Latvia

³ Université du Maine, Laboratoire des Oxydes et Fluorures (UMR 6010 CNRS),

Avenue O. Messiaen, 72085 Le Mans, France

crossref <http://dx.doi.org/10.5755/j01.ms.19.3.2403>

Received 06 September 2012; accepted 13 January 2013

The principle of spark plasma ceramics sintering method is presented, its advantages and disadvantages are discussed. Li⁺ ionic conductor Li_{3x}La_{2/3-x}TiO₃ (x = 0.1) and oxygen ionic conductor CeO₂-20 mol% Sm₂O₃ nanoceramics have been prepared using this method. Electrical properties of the obtained ceramics were measured in the broad frequency range of 10 Hz to 3 GHz and temperature interval from 300 K up to 800 K. Ionic conductivities inside grains and in the grain boundaries have been separated from impedance spectra.

Keywords: solid electrolyte, spark plasma sintering, impedance spectroscopy.

1. INTRODUCTION

Investigation of solid electrolyte nanoceramics is state of the art direction in materials science. Conventional ceramics sintering way is not suitable to create nanoceramics because of grain growth at high sintering temperature. For example in [1] the authors get bigger ceramic crystallites when increasing the sintering temperature. Besides very small grains the obtained ceramics should be of high density, more than 95 % of the theoretical density is necessary for applications. So the preparation of nanoceramics is complicated procedure, which requires special equipment. Spark plasma sintering reactor can be used for this purpose.

Due to very complicated and expensive equipment there are not so many publications about electrical properties of spark plasma sintered solid electrolytes. Yttria stabilized zirconia (YSZ) [2, 3] or several ceria based solid electrolytes [4, 5] have been made and investigated. On the other hand, we have no knowledge about publications where Li⁺ ion conductor was sintered by spark plasma method. So in the present paper the procedure of creating Li_{3x}La_{2/3-x}TiO₃ (x = 0.1) (LLTO) and CeO₂-20 mol% Sm₂O₃ (SDC-20) nanoceramics by spark plasma sintering method is reported, some advantages and disadvantages of the technique is given, and electrical properties of the obtained ceramics have been investigated.

2. EXPERIMENTAL DETAILS

To obtain ceramics with grain sizes in the nanometre range the powders with nanometre particle sizes are required. The preparation procedure of obtaining LLTO nanopowder has already been presented [6]. SDC-20 nanopowder was obtained from Fuel Cell Materials (Lot #: 274-024, surface area: 212 m²/g).

Dr. Sinter spark plasma sintering equipment was used to obtain nanoceramics. 5 g of SDC-20 nanopowder was placed in a graphite press form with 20 mm in diameter and for LLTO 10 mm press form was used. 50 MPa pressure was applied. The simultaneous pressing of the powder in a press form when heated is related to the unique feature of this kind of sintering, namely the possibility to create samples with the preferred geometry. The final sintering temperature of LLTO was 960 °C and it was much lower compared to conventional sintering, which is 1200 °C. Final sintering temperature of SDC-20 was 1100 °C, sintering duration at the highest temperature was 6 min and the whole sintering process lasted only about 10 min. The system had been cooling down naturally for 2 h. The main parameters of SDC-20 sintering process, including temperature, vacuum level in the chamber, applied voltage, current, and shrinkage of the sample in the press form, are shown in Figure 1. We can see from the curves that the last 3 min of the sintering there is no shrinkage of the sample.

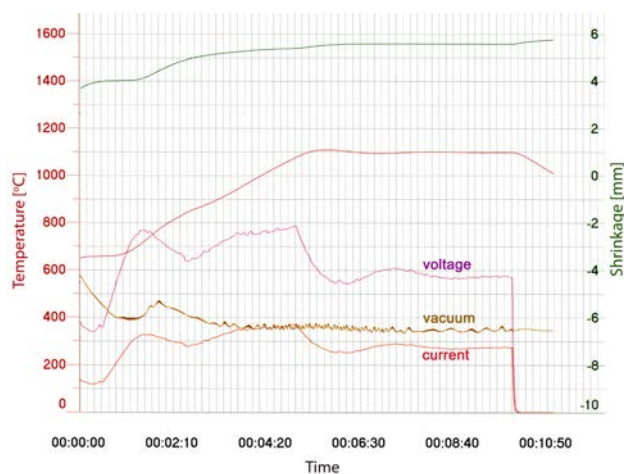


Fig. 1. SDC-20 ceramic spark plasma sintering parameters

* Corresponding author. Tel.: +370-5-2366064; fax.: +370-5-2366064.
E-mail address: tomas.salkus@ff.vu.lt (T. Šalkus)

One of the disadvantages of spark plasma method in case of ionic conductor sintering is the high vacuum during the process. Such conditions lead to reduction of the samples. In SDC Ce^{4+} is reduced to Ce^{3+} and in LLTO Ti^{4+} is reduced to Ti^{3+} . Both materials change colour from light yellow to black. However, these materials can be oxidised back to the initial chemical compositions. The oxidation was performed in air atmosphere at 900 °C, dwell time was 10 h, heating and cooling rates were 3 deg/min. The examples of the samples are shown in Figure 2. Besides the oxidation processes undesirable carbon will burn out from the surface of the obtained samples, which comes from graphite press form.

Unfortunately the sample can crack during cooling in some cases (Figure 2, b) because of different expansion coefficients of graphite and sintered body.

Scanning electron micrographs of LLTO surface show very dense microstructure of the ceramics (Figure 2, c). The nanometric grains do not grow during sintering and remain not bigger than ~100 nm.

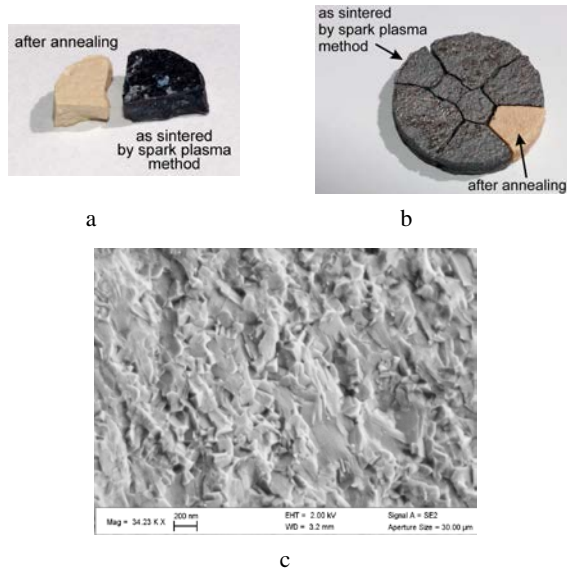


Fig. 2. Colour changes of LLTO (a) and SDC-20 (b) samples as a result of oxidation and reduction reactions, SEM image of LLTO surface (c)

The densities of the obtained ceramics were measured by Archimedes method using analytical electronic balance (KERN & Sohn GmbH, ABS 120-4). The densities of oxidized ceramics were calculated from the formula:

$$\rho = \rho_{H_2O} \frac{m_{in\ air}}{m_{in\ air} - m_{in\ H_2O}}, \quad (1)$$

where ρ_{H_2O} is the density of water (at 23 °C), $m_{in\ air}$ is ceramics weight in air and $m_{in\ H_2O}$ is ceramics weight under pure water. The density of SDC-20 ceramics sintered by spark plasma method was 6.638 g·cm⁻³ and reached 93 % of the theoretical density. The density of LLTO ceramics was 4.569 g·cm⁻³ and reached 91 % of the theoretical density.

Electrical properties of the samples have been measured by two impedance spectrometers. The measurements in the low frequencies from 10 Hz to 2 MHz have been performed

with a home-made impedance spectrometer [7]. In the frequency range 300 kHz – 3 GHz electrical properties of the samples were measured using coaxial technique [8]. Measurement temperature range was from 300 K to 800 K.

3. RESULTS

Frequency dependences of the real part of conductivity (σ') for LLTO and SDC nanoceramics obtained by spark plasma method are shown in Figure 3, a and b, respectively.

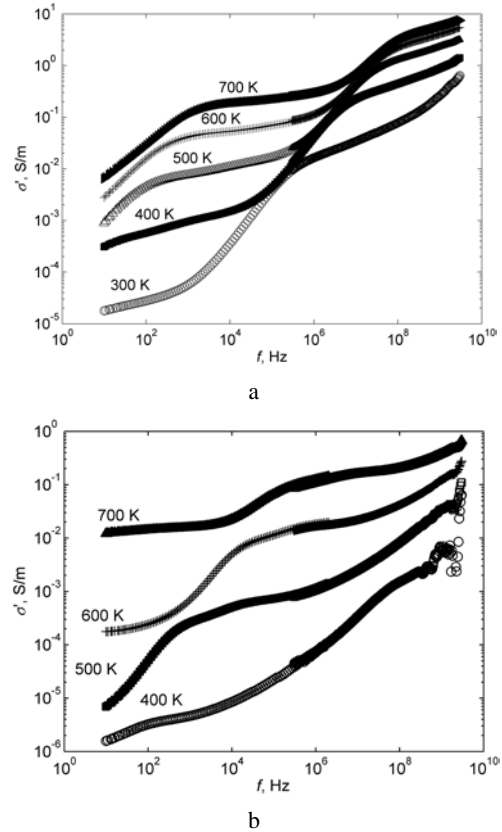


Fig. 3. Frequency dependences of the real part of electrical conductivity in LLTO (a) and SDC-20 (b) at different temperatures

Three dispersive regimes can be observed in the spectrum. The dispersion at the highest frequencies (for example higher than 10⁸ Hz at 300 K for LLTO) is related to ion motion in the ceramic grains, Li⁺ in LLTO and O²⁻ in SDC. At intermediate frequencies dispersion should be associated with ionic transport in the grain boundaries. At the lowest frequencies a clear Pt electrode blocking effect can be observed for LLTO – rapid conductivity decrease at temperatures higher than 500 K. On the other hand, Pt electrode is not fully blocking on oxygen ion conductor SDC-20. So electrode polarization plateau can be seen at high temperatures and low frequencies in Figure 3, b.

Although clear plateaus are absent in the σ' frequency dependences, the grain conductivity can be separated from the total conductivity when fitting the experimental results to an equivalent circuit. The usual representation of the obtained result is complex plain plot. Resistivity in complex plain is presented in Figure 4. Two depressed and partially overlapping semicircles were found and they can

be associated with the resistances of grains and grain boundaries. The diameters of the semicircles correspond to values of $1/\sigma_b$ (“b” denotes grain or “bulk”, as bulk conductivity consists of all grains in the sample) and $1/\sigma_{gb}$ (“gb” denotes “grain boundary”) as it is shown in Figure 4.

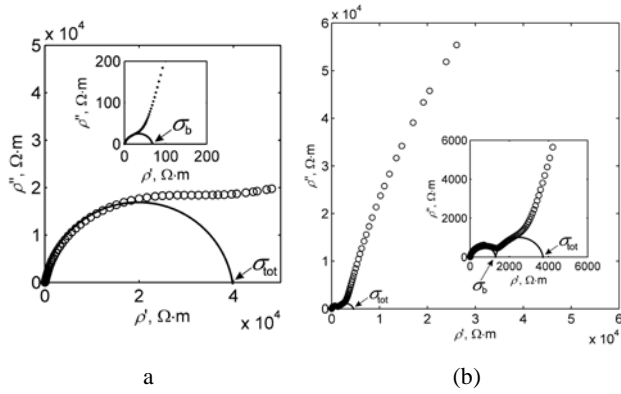


Fig. 4. Complex resistivity plots of LLTO (a) at 300 K and SDC-20 (b) at 500 K, showing bulk (in the inserts) and total conductivities of the ceramics. Solid lines are guides for the eye. Arrows mark the points where the values of conductivities were found from

After analyzing complex resistivity plots at different temperatures, temperature dependences of bulk and total conductivities of LLTO and SDC-20 nanoceramic samples were obtained (Figure 5).

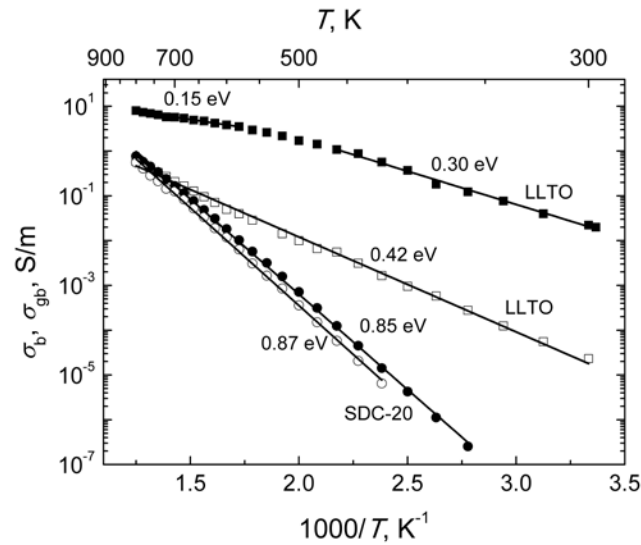


Fig. 5. Arrhenius bulk (full symbols) and total (open symbols) conductivities plots of LLTO (squares) and SDC-20 (circles) nanoceramics. Corresponding conductivity activation energies are presented

The conductivities of ceramics, bulk and total, obey Arrhenius law with one exception. LLTO ceramics activation energy of bulk conductivity changes at about 500 K. Such non-Arrhenius behavior was observed and analyzed previously [9].

Total conductivity is a product of grain (or bulk) and grain boundary resistivities:

$$\sigma_{tot} = \frac{1}{\rho_b + \rho_{gb}}. \quad (2)$$

σ_{tot} of LLTO nanoceramics was found to be several orders of magnitude lower compared to the bulk conductivity. So the major role in the overall LLTO conductivity is played by the non-conductive grain boundaries. Temperature behavior of nano LLTO σ_b is similar to the ceramics with micrometric grains. σ_{tot} activation energies of nano and micro LLTO ceramics are similar, but we have found σ_{tot} values of nano LLTO much lower compared to micro LLTO [9]. Obviously in nanoceramics there are more grain boundaries and they have bigger influence on the electrical properties compared to ceramics with grain sizes in micrometer range.

On the other hand, bulk conductivity of SDC-20 nanoceramics is very close to the total. σ_b and its activation energy is very close to SDC-20 ceramics with micro grains (bulk activation energy is about 0.8 eV), but the values of σ_{gb} and its activation energy strongly depend on ceramics sintering conditions [10]. For the ceramics sintered at temperatures between 1200 °C and 1500 °C grain boundary activation energies vary from about 1.35 eV to 1.03 eV [10]. We have found the grain boundary activation energy of SDC-20 nanoceramics 0.87 eV, which is lower compared to the one of microceramics. This points out, that in SDC-20 the energy barriers for oxygen-ion jumps in grain boundary areas are reduced because of the nanosizes of ceramic grains. Grain boundary properties of oxygen ion conducting solid electrolytes were summarized in the review article of Xin Guo et al. [11]. The nature of oxygen conduction in ceria based solid electrolytes is completely different compared to lithium conductors. At the interfaces between ceramic grains defect concentration is higher, in these regions oxygen vacancies are generated hereby increasing the mobility of O^{2-} ions. So increasing the number of grain boundaries in oxygen conducting ceramics makes grain boundary resistance almost negligible.

4. CONCLUSIONS

$Li_{3x}La_{2/3-x}TiO_3$ ($x = 0.1$) and $CeO_{2-20} mol\% Sm_2O_3$ nanoceramics have been prepared by spark plasma sintering method. The spark plasma sintering offers some essential advantages over conventional ceramic sintering: 1. No grain growth; 2. Good density of the obtained ceramics; 3. Lower sintering temperatures and very fast process. There are also some disadvantages of this process: 1. Reduction of the samples, which need to be oxidised back; 2. Sample pollution with carbon; 3. Sample cracking; 4. Complicated and expensive equipment.

Electrical properties of the obtained ceramics have been investigated by impedance spectroscopy. Ionic conductivities in grains and in grain boundaries of the ceramics were separated from the wide frequency range spectra. The total conductivity of SDC-20 nanoceramics is very close to the bulk conductivity showing grain boundary conduction nature in oxygen conducting ceramics. Contrary, in LLTO nanoceramics the bulk conductivity is several orders of magnitude greater compared to the total conductivity. This property is characteristic to ceramics in which grain boundaries block ionic motion. Non-Arrhenius behaviour is observed in bulk ionic conductivity of LLTO nanoceramics, similarly to the microceramic systems.

Acknowledgments

This research was funded by a grant No. ATE-09/2012 from the Research Council of Lithuania. Tomas Šalkus wishes to acknowledge Research Council of Lithuania for funding this work according to the project "Postdoctoral Fellowship Implementation in Lithuania".

REFERENCES

1. **Bohnke, O.** The Fast Lithium-ion Conducting Oxides $\text{Li}_{3-x}\text{La}_{2/3-x}\text{TiO}_3$ from Fundamentals to Application *Solid State Ionics* 179 2008: pp. 9–15.
2. **Bangchao, Y., Jiawen, J., Yican, Z.** Spark-plasma Sintering the 8-mol% Yttria-stabilized Zirconia Electrolyte *Journal of Materials Science* 39 2004: pp. 6863–6865. <http://dx.doi.org/10.1023/B:JMSSC.0000045622.65071.3d>
3. **Khor, K. A., Yu, L.-G., Chan, S. H., Chen, X. J.** Densification of Spark Plasma Sprayed YSZ Electrolytes by Spark Plasma Sintering (SPS) *Journal of the European Ceramic Society* 23 2003: pp. 1855–1863. [http://dx.doi.org/10.1016/S0955-2219\(02\)00421-1](http://dx.doi.org/10.1016/S0955-2219(02)00421-1)
4. **Anselmi-Tamburini, U., Maglia, F., Chiodelli, G., Tacca, A., Spinolo, G., Riello, P., Bucella, S., Munir, Z.A.** Nanoscale Effects on the Ionic Conductivity of Highly Doped Bulk Nanometric Cerium Oxide *Advanced Functional Materials* 16 2006: pp. 2363–2368.
5. **Plapcianu, C., Valsangiacom, C., Schaffer, J. E., Wieg, A., Garay, J., Stanciu, L.** Spark Plasma Sintering Studies of Nanosize Lanthanide-doped Ceria Obtained by Sol-gel Method *Journal of Optoelectronics and Advanced Materials* 13 (9) 2011: pp. 1101–1108.
6. **Boulant, A., Emery, J., Jouanneaux, A., Buzaré, J.-Y., Bardeau, J.-F.** From Micro- to Nanostructured Fast Ionic Conductor $\text{Li}_{0.30}\text{La}_{0.56}\text{TiO}_3$: Size Effects on NMR Properties *The Journal of Physical Chemistry C* 115 2011: pp. 15575–15585. <http://dx.doi.org/10.1021/jp2048794>
7. **Kežionis, A., Butvilas, P., Šalkus, T., Kazlauskas, S., Petrulionis, D., Žukauskas, T., Kazakevičius, E., Orliukas, A. F.** Four-electrode Impedance Spectrometer for Investigation of Solid Ion Conductors *Review of Scientific Instruments* 84 2013: p. 013902. <http://dx.doi.org/10.1063/1.4774391>
8. **Kežionis, A., Kazakevičius, E., Šalkus, T., Orliukas, A.** Broadband High Frequency Impedance Spectrometer with Working Temperatures up to 1200 K *Solid State Ionics* 188 2011: pp. 110–113. <http://dx.doi.org/10.1016/j.ssi.2010.09.034>
9. **Šalkus, T., Kazakevičius, E., Kežionis, A., Orliukas, A. F., Badot, J. C., Bohnke, O.** Determination of the Non-Arrhenius Behaviour of the Bulk Conductivity of Fast Ionic Conductors LLTO at High Temperature *Solid State Ionics* 188 2011: pp. 69–72.
10. **Min Chen, Bok Hee Kim, Qing Xu, Byeong Kuk Ahn, Woo Jin Kang, Duan Ping Huang.** Synthesis and Electrical Properties of $\text{Ce}_{0.8}\text{Sm}_{0.2}\text{O}_{1.9}$ Ceramics for IT-SOFC Electrolytes by Urea-combustion Technique *Ceramics International* 35 2009: pp. 1335–1343.
11. **Guo, X., Waser, R.** Electrical Properties of the Grain Boundaries of Oxygen Ion Conductors: Acceptor-doped Zirconia and Ceria *Progress in Materials Science* 51 2006: pp. 157–210.